



Full Length Article

Investigation on the Metabolism of Salvianolic acid B, Tanshinone IIA, Ginsenoside Rg1 and Ginsenoside Rb1 from Danshen-Sanqi Herbal Pair in Zebrafish by Liquid Chromatography-Tandem Mass Spectrometry Analysis

Shijun Yin^a, Congpeng Zhao^a, Guang Hu^b, Hua Chen^{a,**}, Fengqing Yang^{a,*}

^a School of Chemistry and Chemical Engineering, Chongqing University, Chongqing 401331, China

^b School of Pharmacy and Bioengineering, Chongqing University of Technology, Chongqing 400054, China



ARTICLE INFO

Keywords:

Zebrafish
Danshen-Sanqi herbal pair
Metabolite
Metabolic pathways
Synergistic effect

ABSTRACT

Background: Salvianolic acid B (SAB), tanshinone IIA (TIIA), ginsenoside Rg1 (GRg1) and ginsenoside Rb1 (GRb1) are the main active components of Danshen-Sanqi herbal pair (DS-SQ), which is widely used in the treatment of cardiovascular diseases in Asia. The compatibility mechanisms of compound Chinese herbal preparation may be clarified to some degree by understanding the interactions of the active components based on their metabolic research. Furthermore, zebrafish is a convenient and feasible model to study the metabolism of drugs.

Objective: To investigate the metabolism of SAB, TIIA, GRg1 and GRb1 in zebrafish by liquid chromatography-tandem mass spectrometry (LC-MS/MS) analysis.

Methods: Zebrafish embryos after 48-hour hatching were divided into nine experimental groups. The blank group was exposed to 1 mL ultra-pure water. Eight drug-treated groups were exposed to 1 mL solution of SAB, TIIA, GRg1, GRb1, SAB and GRg1, SAB and GRb1, TIIA and GRg1, TIIA and GRb1, respectively. After homogenization, they were analyzed by LC-MS/MS. The Structures of the metabolites were determined by analyzing their corresponding mass spectra information and comparing the data with relevant literature. According to the change of the amount of metabolites, the metabolic effect between SAB, TIIA, GRg1 and GRb1 were investigated.

Results: Eighteen metabolites and four parent drugs of SAB, TIIA, GRg1 and GRb1 in zebrafish were identified by LC-MS/MS, including methylation, degradation, reduction, dehydrogenation, hydroxylation, desugarization and glucuronidation metabolites. Furthermore, after being combined exposed of drugs, GRg1 and GRb1 could promote the metabolism of TIIA, while SAB and TIIA could promote the metabolism of GRg1 and GRb1 to different degree.

Conclusion: By using LC-MS/MS analysis, zebrafish was successfully applied to study the metabolism of SAB, TIIA, GRg1 and GRb1, which is significance to explain the possible synergistic effect of components in DS-SQ through modifying the metabolism in zebrafish. This study can be helpful for the further research of DS-SQ.

1. Introduction

Fufang Danshen prescription (FDP), an herbal compound preparation consisting of *Salvia miltiorrhiza* and *Panax notoginseng*, is one of the most widely used drugs for the treatment of cardiovascular diseases in Asia (Liu and Huang, 2016). In vivo and in vitro studies showed that FDP had various biological activities, including alleviating pain (Sun and Yang, 2019), anti-hypoxia (Zeng et al., 2006), reducing cerebral ischemia reperfusion injury (Liang et al. 2013), protecting

endothelial cells from impaired cellular injury (Zhou et al. 2019) and treating coronary heart disease (Guo et al. 2019). A study revealed that Danshen-Sanqi Herbal Pair (DS-SQ) at ratios of 2:8 and 3:7 potentiated angiogenic synergistic effects in EAhy 926 cells (Zhou et al. 2017). Liu et al. confirmed that DS-SQ with a ratio of 10:3 could markedly inhibit platelet aggregation and adhesion in normal rabbit (Liu et al. 2002). Furthermore, the active components from different herbs might interact with each other during the metabolic process, which could potentially influence their therapeutic benefits. In addition, the compatibility

* Corresponding Author: Fengqing Yang, E-mail addresses: fengqingyang@cqu.edu.cn (F. Yang).

Hua Chen, E-mail addresses: chenhuacq@cqu.edu.cn (H. Chen).

mechanisms of compound Chinese herbal preparation might be clarified to some degree by understanding the interaction of the active components based on their metabolic research (Huang et al. 2016). Therefore, it is of significant importance to clarify the *in vivo* metabolism and metabolic effect of the representative active components of DS-SQ.

Zebrafish, which have the characteristics of small size, fast reproduction, transparent embryos and short experimental period, were widely used in genetics, developmental biology, human disease research and drug safety evaluation (Bhattacharya et al. 2018; Falcão et al. 2018). The zebrafish and human genetic sequences have more than 50% homology, and zebrafish can express a variety of drug-metabolizing enzymes, such as phase I enzymes cytochrome P450 (CYP) and phase II enzymes UDP-glucuronosyltransferases and sulfotransferases (Wang et al. 2018; Bašica et al. 2019). Therefore, the studies of zebrafish for drug metabolisms are receiving more and more attentions (Yan et al. 2019; Benchoula et al. 2019). The hydroxylated metabolite had been detected after exposure the zebrafish to the ibuprofen solution for 24 h, which indicated that zebrafish could metabolize ibuprofen in a mammalian CYP450 zymogen-like manner (Jones et al. 2012). In our recent study, the conjugative activities had been confirmed by detecting glucuronidation metabolites of curcumin and baicalein in zebrafish (Yin et al. 2020).

Salvianolic acid B (SAB) and (tanshinone IIA (TIIA) are the main phenolic acids and quinones in Danshen (Yang et al. 2015), respectively. Ginsenoside Rb1 (GRb1) and ginsenoside Rg1 (GRg1) are the main protopanaxadiol and protopanaxatriol in Sanqi (Liu et al. 2009), respectively. Furthermore, these compounds have significant pharmacological activity on the treatment of cardiovascular diseases. In addition, TIIA, SAB and GRg1 have been used as quality control markers for FDP in Chinese Pharmacopoeia. Therefore, in this work, SAB, TIIA, GRb1 and GRg1 were selected as the representative active compounds, owing to their various pharmacological activities and high contents in the herbs (Xu et al. 2019; Pang et al. 2016). The metabolisms of SAB, TIIA, GRb1 and GRg1 in zebrafish were investigated by high-performance liquid chromatography combined with triple-quadruple mass spectrometer. In addition, the metabolic effect among those four investigated compounds was explored according to the change of amount of their metabolites.

2. Materials and Methods

2.1. Chemicals and Reagents

Ginsenoside Rg1 and Ginsenoside Rb1 were purchased from Shanghai Yuanye Biotechnology Co., Ltd. ($\geq 98.0\%$, Shanghai, China). Salvianolic acid B was purchased from PureChem-Standard Co., Ltd. ($\geq 98.0\%$, Chengdu, China). Tanshinone IIA was purchased from Beijing Solarbio Scientific Co., Ltd. ($\geq 98.0\%$, Beijing, China). Dimethyl sulfoxide (DMSO) was purchased from Chengdu Chron Chemicals Co., Ltd. (Chengdu, China). Acetonitrile (HPLC grade) and formic acid (HPLC grade) were obtained from Beijing InnoChem Science & Technology Co., Ltd. (Beijing, China). All of the experimental water was purified by a water purification system (ATSelem 1820A, Antesheng Environmental Protection Equipment Co., Ltd., Chongqing, China). Buffers and samples were ultrasonicated in a KQ-100B ultrasonic cleaner (Kunshan ultrasonic instruments Co., Ltd., Kunshan, China) before use.

2.2. LC-MS/MS analysis

The analysis of metabolites were conducted on a Shimadzu 8060 Triple-Quadruple mass spectrometer (Shimadzu, Kyoto, Japan) equipped with ESI interface that was connected to a HPLC system. The mobile phase consisted of solvent A (0.1% formic acid aqueous solution) and solvent B (acetonitrile) using a gradient elution program: 7%-27% B at 0-10 min, 27%-35% B at 10-25 min, 35%-65% B at 25-37 min, 65%-80% B at 37-50 min, 80%-7% B at 50-55 min, 7% B at 55-60 min. The flow rate was 1.0 mL/min. An Agilent Zorbax SB-Aq column

(250 × 4.6 mm, 5 μ m) maintained at 30°C was used for separation. The injection volume of sample was 10 μ L.

The ESI-MS conditions were as follows: drying gas pressure, 100 MPa; curved desolvation line (CDL) voltage, constant level; interface voltage, 1.4 kV; nebulizing gas flow rate, 3 L/min; detector voltage, 1.40 kV; CDL temperature, 250°C; block heater temperature, 400°C; and vacuum, 1.9×10^{-2} Pa. The mass spectra were recorded in simultaneous positive and negative ionization full-scan mode with the m/z range of 100-2000. The ion accumulation time was set at 100 ms and the collision energy of collision induced dissociation (CID) was set at 50%. Data acquisition and processing were performed with the LC-MS solution version 1.1 software (Shimadzu).

2.3. Drug administration and biological sample preparation

The zebrafish were kept under laboratory conditions for three months before experiments. The culture and reproduction of zebrafish was carried out by the Westerfield method (Yin et al. 2020). Zebrafish embryos after 48-h hatching were divided into nine experimental groups of thirty larvae each and placed in a 12-hole plate. The blank group G1 was exposed in 1 mL ultra-pure water. Eight drug-treated groups G2-G9 were exposed to solution (8 μ M, 1 mL) of SAB, TIIA, GRg1, GRb1, SAB and GRg1, SAB and GRb1, TIIA and GRg1, TIIA and GRb1, respectively. All the above hatch water contained 0.05% DMSO.

After 48-h hatching, the zebrafish larvae were sucked with a plastic head dropper, and then washed three times using purified water and homogenized. After being centrifuged at $3200 \times g$ for 15 min, the supernatant was collected and 1 mL methanol was added, followed by centrifugation at $2.312 \times 10^4 \times g$ for 15 min to remove protein and tissue pieces. The supernatant liquid was filtrated through 0.45 μ m microporous membrane and analyzed by LC-MS/MS.

2.4. Statistical analysis

The results were presented as mean \pm standard deviations (SD) of three different experiments. The statistical analysis was performed with SPSS (version 24, SPSS, Inc., Chicago, IL, USA).

3. Results and Discussion

3.1. Identification of SAB, TIIA, GRg1 and GRb1 metabolites after zebrafish exposure

SAB, TIIA, GRg1 and GRb1 and their metabolites after zebrafish exposure were identified by HPLC-MS/MS in simultaneous negative and positive mode. By comparing the total ion chromatograms (TICs) of blank group and drug treated group (Fig. S1), and comparing the fragmentation behaviors and retention time with reference data and some of reference compounds, eighteen metabolites and four prototypes of SAB, TIIA, GRg1 and GRb1 were identified in the drug-containing samples. The retention time, metabolic type and major product ions were summarized in Table 1.

3.1.1. Identification of SAB metabolites

Seven metabolites and parent component of SAB were detected in both zebrafish body and zebrafish solution. The related MS and MS² spectra of metabolites and the parent compound were given in the Fig. S2 and Fig. S3. SAB was identified as it showed the deprotonated molecule $[M-H]^-$ at m/z 717 and the product ion at m/z 679 $[M-H-2H_2O-2H]^-$ (Zeng et al. 2006). SAB-1 showed the quasi-molecular $[M-H]^-$ ion at m/z 731, 14 Da higher than that of SAB, suggesting that SAB-1 was monomethyl-SAB (Qi et al. 2013). The $[M-H]^-$ and the product ion of SAB-2 were at m/z 197 and m/z 153 $[M-H-COOH]^-$, respectively, indicating that SAB-2 was tanshinol (Meng et al. 2019). SAB-5 was observed as quasi-molecular $[M-H]^-$ ion at m/z 537, which might be resulted from the loss of caffeic acid (CA, 180 Da), SAB-5

Table 1
Identification of the metabolites of SAB, TIIA, GRg1 and GRb1 in zebrafish by HPLC-MS/MS

Metabolite	Retention time t_R (min)	Reaction type	MS (m/z)	Identification	Incubation solution	Zebrafish body
SAB	11.996		717 ([M-H] ⁻), 679 ([M-H-2H ₂ O-2H] ⁻), 468	SAB	+ ^a	+
SAB-1	2.057	methylation	731 ([M-H] ⁻), 557	Monomethyl-SAB	+	+
SAB-2	8.673	degradation	197 ([M-H] ⁻), 153 ([M-H-CO ₂] ⁻)	Tanshinol	+	+
SAB-3	10.882	degradation methylation	551 ([M-H] ⁻), 432, 325 ([M-H-DSS-CO] ⁻), 297 ([M-H-DSS-2CO] ⁻)	Monomethyl-LSA	+	+
SAB-4	42.313		361 ([M-H] ⁻)	SAR ^c	+	+
SAB-5	44.691	degradation	537 ([M-H] ⁻), 423, 339 ([M-H-DSS] ⁻)	LSA	+	+
SAB-6	51.167	degradation	539 ([M-H] ⁻), 325 ([M-H-CA-CH ₃ -H ₂ O-H] ⁻)	SAS	+	+
SAB-7	52.878	degradation	165 ([M-H] ⁻), 148 ([M-H-OH] ⁻)	3-(3-hydroxyphenyl)-propionic acid	+	+
TIIA	49.449		317 ([M+Na] ⁺), 295 ([M+H] ⁺), 280 ([M+H-CH ₃] ⁺), 262 ([M+H-CH ₃ -H ₂ O] ⁺), 234 ([M+H-CH ₃ -H ₂ O-CO] ⁺), 219 ([M+H-2CH ₃ -H ₂ O-CO] ⁺)	TIIA	+	+
TIIA -1	2.691	hydroxylation	311 ([M+H] ⁺), 222 ([M+H-3CH ₃ -CO ₂] ⁺), 203 ([M+H-3CH ₃ -COOH-H ₂ O-H] ⁺)	Monohydric-TIIA	+	^b
TIIA -2	9.229	reduction glucuronidation	471 ([M+H] ⁺), 309, 277 ([M+H-glca-H ₂ O] ⁺), 251	Dehydrotanshinone IIA glucuronide	+	+
TIIA -3	9.794	hydroxylation glucuronidation	487 ([M+H] ⁺), 471 ([M+H-OH+H] ⁺), 427 ([M+H-COOH-CH ₃] ⁺), 383 ([M+H-COOH-CO ₂ -CH ₃] ⁺), 365, 295 ([M+H-glca-OH+H] ⁺), 251 ([M+H-glca-OH-CO ₂] ⁺)	Hydroxytanshinone IIA glucuronide	+	+
TIIA -4	10.806	reduction	293 ([M+H] ⁺), 277 ([M+H-CH ₃ -H] ⁺), 233 ([M+H-OH-CO-CH ₃] ⁺), 218 ([M+H-OH-CO-2CH ₃] ⁺)	Dehydrotanshinone IIA	+	+
TIIA -5	13.901	glucuronidation	473 ([M+H] ⁺), 278 ([M+H-glca-H ₂ O-H] ⁺)	Tanshinone IIA glucuronide	+	+
GRg1	42.347		800 ([M-H] ⁻), 313	GRg1	+	-
GRg1-1	49.313	desugarization	684 ([M+HCOO] ⁻)	GF1/GRh1	+	+
GRg1-2	49.174	desugarization	475 ([M-H] ⁻), 137	Ppt	+	+
GRb1	27.825		1132 ([M+Na] ⁺)	GRb1	+	+
GRb1-1	30.920	hydroxylation	1169 ([M+HCOO] ⁻)	GRb1 Monohydric-GRb1	+	+
GRb1-2	39.843	desugarization	992 ([M+HCOO] ⁻), 855	GRd	+	+
GRb1-3	12.623	desugarization	808 ([M+Na] ⁺)	GRg3/GF2	+	+
GRb1-4	50.268	desugarization	645 ([M+Na] ⁺), 407	GRh2	+	+

^a Detectable

^b Undetectable

^c Glca, glucuronic acid; DSS, Danshensu; CA, caffeic acid; SAR, salvianolic acid R; LSA, lithospermic acid; SAS, salvianolic acid S; GF1, Ginsenoside F1; GRh1, Ginsenoside Rh1; Ppt, Protopanaxatriol; GRd, Ginsenoside Rd; GRg3, Ginsenoside Rg3; GRF2, Ginsenoside RF2; GRh2, Ginsenoside Rh2; glc, β -D-glucopyranos

was supposed to be lithospermic acid (LSA) (Wang et al. 2008). The [M-H]⁻ ion of SAB-3 was 14 Da higher than that of SAB-5, suggesting that it might be monomethyl-LSA (Li et al. 2007). The mass spectrum of SAB-4 gives the quasi-molecular at m/z 361, which was assigned to be salvianolic acid R (SAR) (Xu et al. 2007). Mass spectra of SAB-6 give the quasi-molecular [M-H]⁻ ion at m/z 539 and the characteristic fragment ion at m/z 325 [M-H-CA-CH₃-H₂O-H]⁻, indicating the dissociation of ester bond, so SAB-6 was supposed to be salvianolic acid S (SAS) (Xu et al. 2007). SAB-7 was the degradation of SAB based the quasi-molecular [M-H]⁻ ion at m/z 165 and the characteristic fragment ion at m/z 148 [M-H-OH]⁻, SAB-7 was supposed to be 3-(3-hydroxyphenyl)-propionic acid (Xu et al. 2007). The proposed biotransformation pathway of SAB in zebrafish was shown in Fig. 1.

3.1.2. Identification of TIIA metabolites

The total ion chromatogram and extracted mass chromatograms of TIIA in zebrafish was shown in Fig. S4, and the MS² spectra were shown in Fig. S5. TIIA was identified by the protonated molecule [M+H]⁺ at m/z 295 and quasi-molecular [M+Na]⁺ ion at m/z 317, the fragment ion at m/z 280 formed by the loss of 15 Da (CH₃) from the precursor ion m/z 295, as well as the fragment ion at m/z 262 and m/z 234 formed by the loss of 18 Da (H₂O) and 28 Da (CO) from m/z 280, respectively (Li et al., 2006). TIIA-1 gives quasi-molecular [M+H]⁺ and [M+Na]⁺ at m/z 311 and 333, both of which were 16 Da higher than that of TIIA, indicating that TIIA-1 might be hydroxyl metabolite of TIIA (Li et al. 2006). The fragment ions of TIIA-2 were similar to those of TIIA-4 except for the neutral loss of 176 Da. Therefore, TIIA-2 was supposed to be the glucuronide conjugate of TIIA-4 (Zhao et al. 2018). TIIA-3 gives the

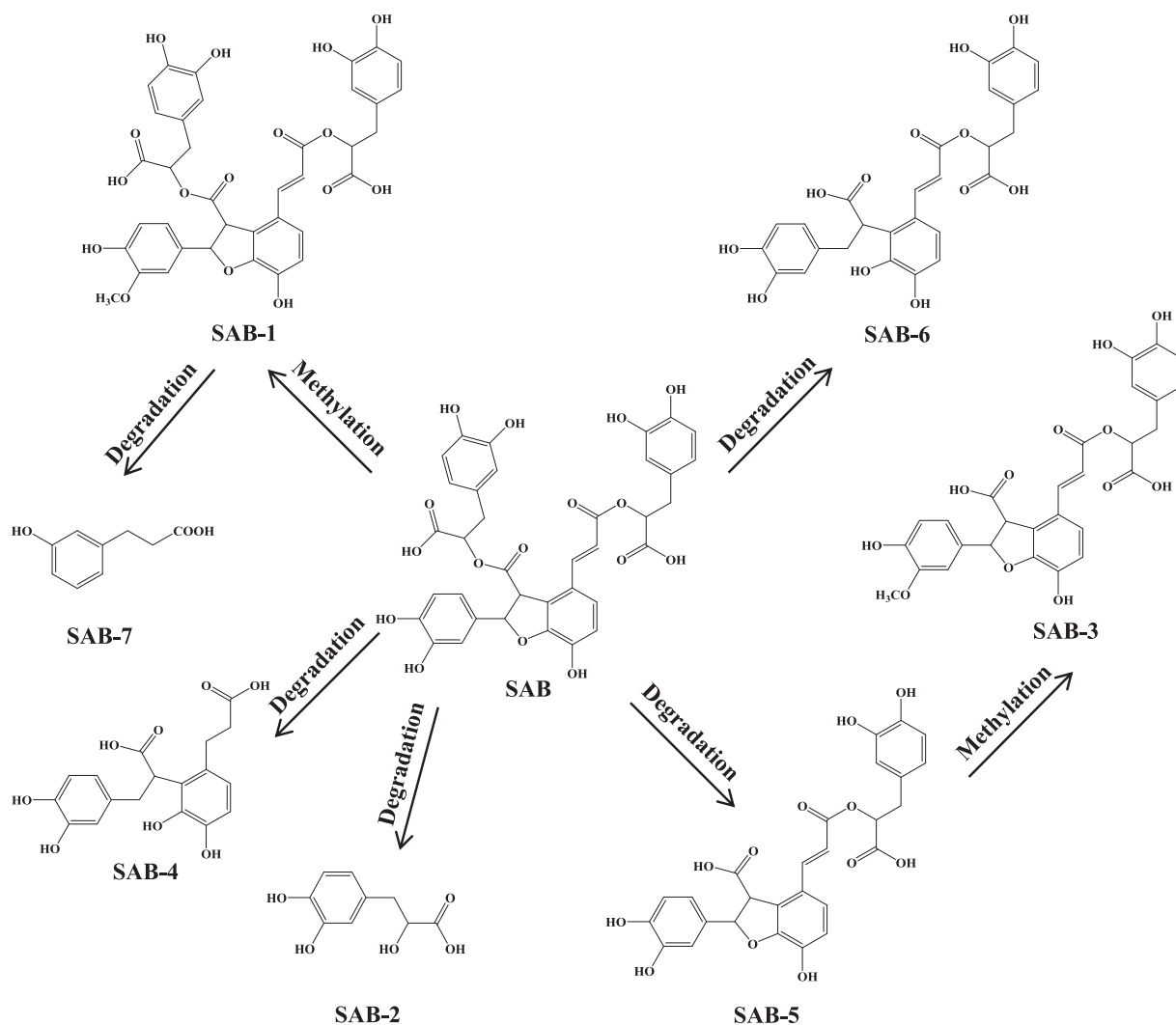


Fig. 1. Proposed biotransformation pathways of SAB in zebrafish.

protonated molecule $[M+H]^+$ at m/z 487 and could be detected by the neutral loss scan of 176 Da, indicating that TIIA-3 was the glucuronide conjugate of the hydroxyl metabolite of TIIA (Wei et al. 2012). TIIA-4 gives the protonated molecule $[M+H]^+$ at m/z 293, which was only 2 Da less than TIIA. It was supposed to be a dehydrogenated product of TIIA (Hao et al. 2006). Tanshinone IIA glucuronide (TIIA-5) was observed as its glucuronide conjugated protonated molecule $[M+H]^+$ at m/z 473 (Li et al. 2006). The proposed metabolic pathway of TIIA was presented in Fig. 2.

3.1.3. Identification of GRg1 metabolites

Two deglycosylated metabolites and parent drug of GRg1 were detected in both zebrafish body and solution, the related MS and MS² spectra were given in the Fig. S6 and Fig. S7. GRg1 was observed as its protonated molecule $[M-H]^-$ at m/z 800 (He et al. 2016). GRg1-1 and GRg1-2 showed quasi-molecular $[M+Na]^+$ ion at m/z 662 and $[M-H]^-$ at m/z 475, indicating the neutral losses of one or two glucose from GRg1, respectively. Therefore, GRg1-1 and GRg1-2 were supposed to be the mono-deglycosylated metabolites Rh1/F1 and di-deglycosylated metabolites Protopanaxatriol (Ppt) (Chen et al. 2015; Wang et al. 2016; Wang et al. 2014), respectively. The proposed metabolic pathway of GRg1 in zebrafish was shown in Fig. 3.

3.1.4. Identification of GRb1 metabolites

Four hydroxylation and desugarization metabolites of GRb1 were detected from both zebrafish body and solution, the related MS and MS² spectra were given in the Fig. S8 and Fig. S9. GRb1 was identified by its quasi-molecular $[M+Na]^+$ at m/z 1132 (Yu et al. 2017). GRb1-1 gave the quasi-molecular $[M+HCOO]^-$ at m/z 1170 and could be detected by the neutral loss of 16 Da, indicating that GRb1-1 was the hydroxyl metabolite of GRb1 (Yu et al. 2017). GRb1-2, GRb1-3 and GRb1-4 were observed as quasi-molecular $[M+HCOO]^-$ at m/z 992, $[M+Na]^+$ at m/z 808 and $[M+Na]^+$ at m/z 645, which were 162 Da, 324 Da and 486 Da higher than that of GRb1, indicating that they might be desugarization metabolites of GRb1. Therefore, GRb1-2, GRb1-3 and GRb1-4 were tentatively identified as GRd, GRg3/GF2 and GRh2, respectively (Kang et al. 2016; Wang et al. 2015; Kang et al. 2015). The proposed metabolic pathway of GRb1 was presented in Fig. 4.

3.2. Metabolic interaction effects of SAB, TIIA, GRg1 and GRb1 in zebrafish

In order to investigate the metabolic interaction effects of SAB, TIIA, GRg1 and GRb1 in zebrafish, the amount of parent drugs and metabolites after single and combined exposure were determined by the change of corresponding peak area. The results were shown in Fig. 5. It was found that GRg1 and GRb1 could reduce the amount of SAB-1 and SAB-5 significantly, but increase the amount of SAB-3, SAB-6

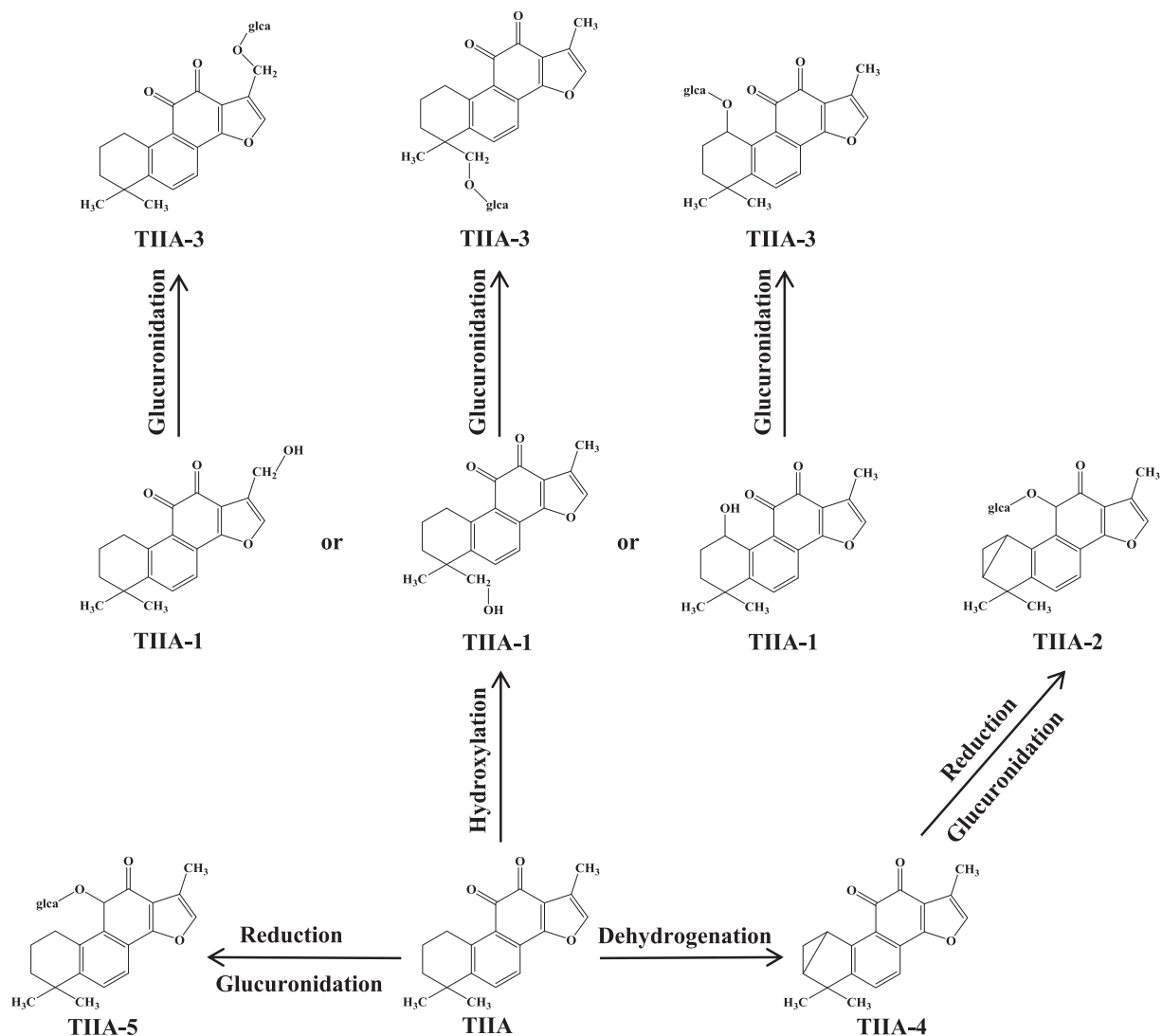


Fig. 2. Proposed biotransformation pathways of TIIA in zebrafish.

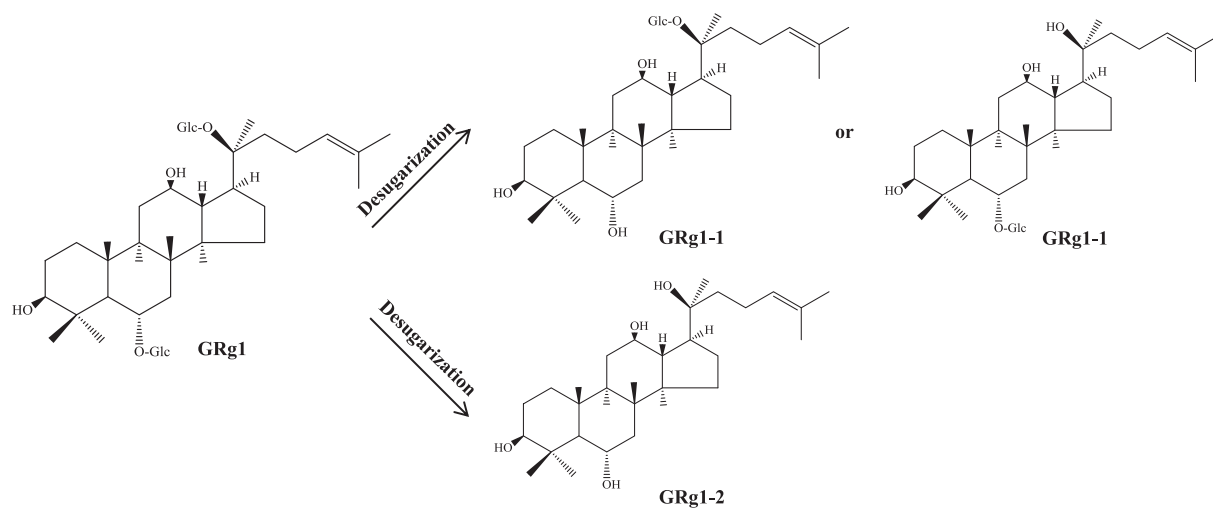


Fig. 3. Proposed biotransformation pathways of GRg1 in zebrafish.

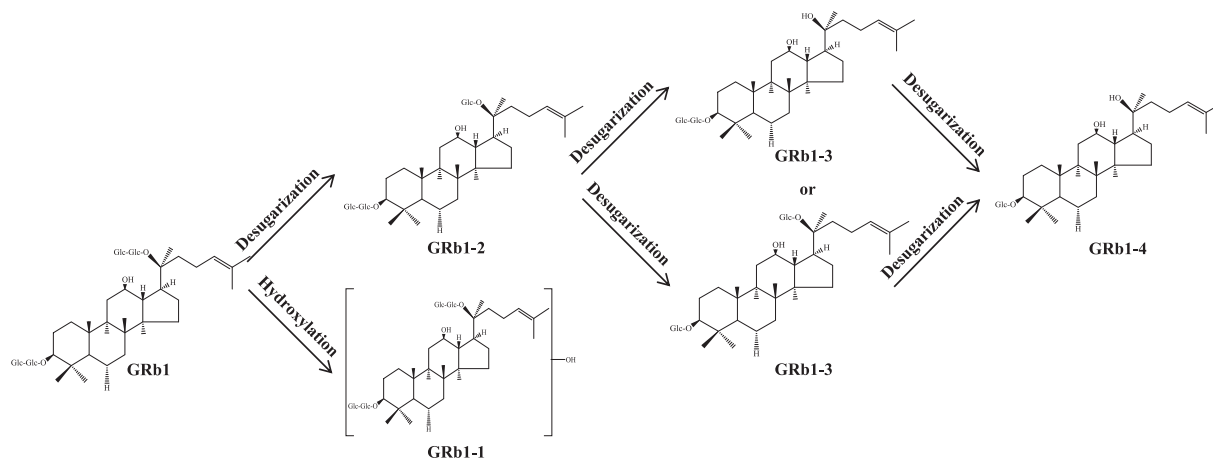


Fig. 4. Proposed biotransformation pathways of GRb1 in zebrafish.

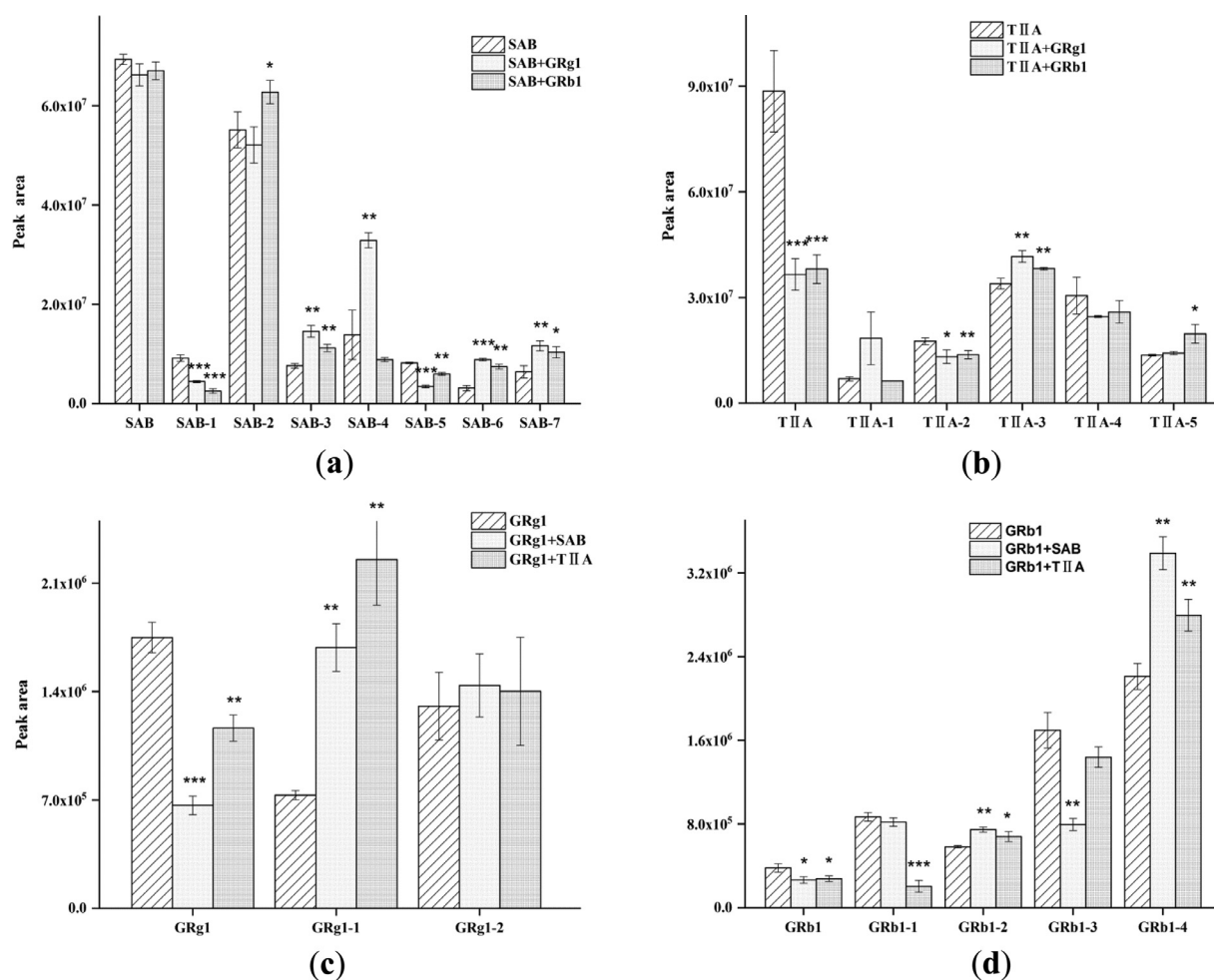


Fig. 5. The peak areas of SAB (a), TIIA (b), GRg1 (c) and GRb1 (d) metabolites after single and combined exposure to zebrafish (n=3). Each error bar represents the standard error of the mean (SEM); *, significantly changed compare with group of single administration (p<0.05); **, significantly changed compare with group of single administration (p<0.01); ***, significantly changed compare with group of single administration (p<0.001)

and SAB-7. As for TIIA, the amount of TIIA and TIIA-2 were significantly decreased, but the amount of TIIA-3 increased after co-treating with GRg1 and GRb1. For GRg1 and GRb1, the amount of GRg1 and GRb1 decreased, but the amount of GRg1-1, GRb1-2 and GRb1-4 was increased with different degree after combining exposure with SAB and TIIA. These results indicated that the interaction effect of the main

active components of *Salvia miltiorrhiza* and *Panax notoginseng* may be due to the change of the metabolic levels. The content-increasing metabolites have achieved considerable attention as promising adjunct and supportive agents in the prevention and treatment of cardiovascular disease. Numerous previous studies have demonstrated that ginsenoside F1 could increase the cerebral microvessel density and promotes angio-

genesis in vitro and in vivo via activating the insulin-like growth factor 1/insulin-like growth factor 1 receptor pathway in endothelial cells (Zhang et al. 2019). Furthermore, ginsenoside F1 decrease endothelial cell apoptosis, alleviate inflammation in endothelial cells, prevent from the adherence of monocytes to endothelial cells, and postpone the progression of atherosclerosis by activating A20-mediated NF- κ B pathway (Qin et al. 2017). Ginsenoside Rd showed protective effect against myocardial ischemic/reperfusion injury via modulation of Akt/GSK and Nrf₂/HO-1 signalling pathways (Zeng et al. 2015). Moreover, Ginsenoside Rd could alleviate operation-induced cardiac hypertrophy through inhibition of oxidative stress, mitogen-activated protein kinase signaling pathway and inflammation (Zhang et al., 2019). The metabolites of GRg1 and GRb1 are potential anti-tumor drugs based on their favorable efficacy and safety profiles. Ginsenoside Rh2 represses autophagy in cervical cancer cells and enhanced apoptosis through an apoptosis-inducing factor mediated pathway (Wang et al. 2020). In addition, ginsenoside Rh2 could induce apoptosis by promoting mitogen-activated protein kinase signaling pathway and inhibit PI3K/Akt/mTOR and nuclear factor-kappa B signaling pathway in U2OS cells (Li et al. 2020). Therefore, the increased levels of metabolites due to metabolic interactions may have effects on treating human disease.

4. Conclusion

In this study, eighteen metabolites and four parent compounds of SAB, TIIA, GRg1 and GRb1 in zebrafish were detected and tentatively identified by LC-MS/MS. The biotransformation pathways of SAB, TIIA, GRg1 and GRb1 in zebrafish were proposed, including phase I metabolism (methylation, degradation, reduction, dehydrogenation, hydroxylation and desugarization) and phase II metabolism (Glucuronidation). This work proposed a strategy to study the metabolism of the main active components in *Salvia miltiorrhiza* and *Panax notoginseng*, which may partially explain the possible synergistic effect of compounds in DS-SQ through modifying the metabolism in zebrafish.

Ethical Approval

Efforts were made to minimize the number of animals used and their suffering. Animal care and treatment procedures were in accordance with the ethical standards of the institution or practice at which the studies were conducted. All procedures performed in studies involving animals were approved by animal care and use committees where the studies were conducted. This article does not contain any studies with human participants performed by any of the authors.

Declaration of Competing Interest

The authors declare that they have no known competing financial interests or personal relationships that could have appeared to influence the work reported in this paper.

CRedit authorship contribution statement

Shijun Yin: Conceptualization, Methodology, Investigation, Writing – original draft. **Congpeng Zhao:** Investigation. **Guang Hu:** Investigation. **Hua Chen:** Supervision. **Fengqing Yang:** Supervision, Project administration, Funding acquisition.

Acknowledgements

We are grateful to Miss Ya-Li Wang from Chongqing University for her technical help.

ORCID

Feng-Qing Yang, <https://orcid.org/0000-0002-9300-5710>.

Supplementary materials

Supplementary material associated with this article can be found, in the online version, at doi:10.1016/j.ccmp.2021.100001.

References

- Bhattacharya, M, Ghosh, S, Malick, RC, Patra, BC, Das, BK., 2018. Therapeutic applications of zebrafish (*Danio rerio*) miRNAs linked with human diseases: A prospective review. *Gene* 679, 202–211. doi:10.1016/j.gene.2018.09.008.
- Bašica, B, Mihaljević, I, Maraković, N, Kovačević, R, Smital, T., 2019. Molecular characterization of zebrafish Gstr1, the only member of teleost-specific glutathione S-transferase class. *Aquat Toxicol* 208, 196–207. doi:10.1016/j.aquatox.2019.01.005.
- Benchoula, K, Khatib, A, Quzwain, FMC, Che Mohamad, CA, Wan Sulaiman, WMA, Abdul Wahab, R, Ahmed, QU, Abdul Ghaffar, M, Saiman, MZ, Alajmi, MF, El-Seedi, H, 2019. Optimization of hyperglycemic induction in zebrafish and evaluation of its blood glucose level and metabolite fingerprint treated with *Psychotria malayana* Jack leaf extract. *Molecules* 24 (8), E1506. doi:10.3390/molecules24081506.
- Chen, D, Lin, S, Xu, W, Huang, M, Chu, J, Xiao, F, Lin, J, Peng, J, 2015. Qualitative and quantitative analysis of the major constituents in Shexiang Tongxin dropping pill by HPLC-Q-TOF-MS/MS and UPLC-QqQ-MS/MS. *Molecules* 20 (10), 18597–18619. doi:10.3390/molecules201018597.
- Falcão, MAP, de Souza, LS, Dolabella, SS, Guimarães, AG, Walker, CIB., 2018. Zebrafish as an alternative method for determining the embryo toxicity of plant products: a systematic review. *Environ Sci Pollut Res Int* 25 (35), 35015–35026. doi:10.1007/s11356-018-3399-7.
- Guo, MZ, Wang, TY, Yang, J, Chang, H, Ji, S, Tang, DQ, 2019. Interaction of clopidogrel and fufang danshen dripping pills assay in coronary heart disease based on non-target metabolomics. *J Ethnopharmacol* 234, 189–196. doi:10.1016/j.jep.2019.01.030.
- Hao, H, Wang, G, Li, P, Li, J, Ding, Z., 2006. Simultaneous quantification of cryptotanshinone and its active metabolite tanshinone IIA in plasma by liquid chromatography/tandem mass spectrometry (LC-MS/MS). *J Pharm Biomed Anal* 40 (2), 382–388. doi:10.1016/j.jpba.2005.07.029.
- He, C, Feng, R, Sun, Y, Chu, S, Chen, J, Ma, C, Fu, J, Zhao, Z, Huang, M, Shou, J, Li, X, Wang, Y, Hu, J, Wang, Y, Zhang, J., 2016. Simultaneous quantification of ginsenoside Rg1 and its metabolites by HPLC-MS/MS: Rg1 excretion in rat bile, urine and feces. *Acta Pharm Sin B* (6) 593–599. doi:10.1016/j.apsb.2016.05.001.
- Huang, J, Zhang, J, Bai, J, Xu, W, Wu, D, Qiu, X., 2016. LC-MS/MS determination and interaction of the main components from the traditional Chinese drug pair Danshen-Sanqi based on rat intestinal absorption. *Biomed Chromatogr* 30 (12), 1928–1934. doi:10.1002/bmc.3768.
- Jones, HS, Trollope, HT, Hutchinson, TH, Panter, GH, Chipman, JK., 2012. Metabolism of ibuprofen in zebrafish larvae. *Xenobiotica* 42 (11), 1069–1075. doi:10.3109/00498254.2012.684410.
- Kang, A, Zhang, SJ, Shan, JJ., 2015. Gut microbiota-mediated deglycosylation of ginsenoside Rb-1 in rats: in vitro and in vivo insights from quantitative ultra-performance liquid chromatography-mass spectrometry analysis. *Anal Methods* 7 (15), 6173–6181. doi:10.1039/C5AY01098E.
- Kang, A, Zhang, SJ, Zhu, D, Dong, Y, Shan, JJ, Xie, T, Wen, HM, Di, LQ., 2016. Gut microbiota in the pharmacokinetics and colonic deglycosylation metabolism of ginsenoside Rb1 in rats: contrary effects of antimicrobials treatment and restraint stress. *Chem Biol Interact* 258, 187–196. doi:10.1016/j.cbi.2016.09.005.
- Li, CC, Gao, H, Feng, XM, Bi, CY, Zhang, J, Yin, JY., 2020. Ginsenoside Rh2 impedes proliferation and migration and induces apoptosis by regulating NF- κ B, MAPK, and PI3K/Akt/mTOR signaling pathways in osteosarcoma cells. *J Biochem Mol Toxicol* 34 (12), e22597. doi:10.1002/jbt.22597.
- Li, P, Wang, GJ, Li, J, Hao, HP, Zheng, CN., 2006. Characterization of metabolites of tanshinone IIA in rats by liquid chromatography/tandem mass spectrometry. *J Mass Spectrom* 41 (5), 670–684. doi:10.1002/jms.1027.
- Li, P, Wang, GJ, Li, J, Hao, HP, Zheng, CN., 2006. Simultaneous determination of tanshinone IIA and its three hydroxylated metabolites by liquid chromatography/tandem mass spectrometry. *Rapid Commun Mass Spectrom* 20 (5), 815–822. doi:10.1002/rcm.2367.
- Li, X, Yu, C, Wang, L, Lu, Y, Wang, W, Xuan, L, Wang, Y., 2007. Simultaneous determination of lithospermic acid B and its three metabolites by liquid chromatography/tandem mass spectrometry. *J Pharm Biomed Anal* 43 (5), 1864–1868. doi:10.1016/j.jpba.2007.01.004.
- Liang, XY, Li, HN, Yang, XY, Zhou, WY, Niu, JG, Chen, BD., 2013. Effect of Danshen aqueous extract on serum hs-CRP, IL-8, IL-10, TNF- α levels, and IL-10 mRNA, TNF- α mRNA expression levels, cerebral TGF- β 1 positive expression level and its neuroprotective mechanisms in CIR rats. *Mol Biol Rep* 40 (4), 3419–3427. doi:10.1007/s11033-012-2419-9.
- Liu, C, Huang, Y., 2016. Chinese herbal medicine in cardiovascular diseases and the mechanisms of action. *Front Pharmacol* 7, 469. doi:10.1038/s41598-019-40694-4.
- Liu, T, Qin, CL, Zhang, Y, Kang, LY, Sun, YF, Zhang, BL., 2002. Effect of Dan-shen, San-qi of different proportion on platelet aggregation and adhesion in normal rabbits. *Zhongguo Zhong Yao Za Zhi* 27 (8), 609–611.
- Liu, Y, Li, J, He, J, Abliz, Z, Qu, J, Yu, S, Ma, S, Liu, J, Du, D., 2009. Identification of new trace triterpenoid saponins from the roots of *Panax notoginseng* by high-performance liquid chromatography coupled with electrospray ionization tandem mass spectrometry. *Rapid Commun Mass Spectrom* 23 (5), 667–679. doi:10.1002/rcm.3917.
- Meng, X, Jiang, J, Pan, H, Wu, S, Wang, S, Lou, Y, Fan, G., 2019. Preclinical absorption, distribution, metabolism, and excretion of sodium danshensu, one of the main water-soluble ingredients in *Salvia miltiorrhiza*, in rats. *Front Pharmacol* 10, 554. doi:10.3389/fphar.2019.00554.

- Pang, H, Wu, L, Tang, Y, Zhou, G, Qu, C, Duan, JA., 2016. Chemical analysis of the herbal medicine *Salviae miltiorrhizae Radix* et *Rhizoma* (Danshen). *Molecules* 21 (1), 51. doi:10.3390/molecules21010051.
- Qi, Q, Hao, K, Li, FY, Cao, LJ, Wang, GJ, Hao, HP., 2013. The identification and pharmacokinetic studies of metabolites of salvianolic acid B after intravenous administration in rats. *Chin J Nat Med* 11 (5), 560–565. doi:10.1016/S1875-5364(13)60101-6.
- Qin, M, Luo, Y, Lu, S, Sun, J, Yang, K, Sun, GB, Sun, XB., 2017. Ginsenoside F1 ameliorates endothelial cell inflammatory injury and prevents atherosclerosis in mice through A20-mediated suppression of NF- κ B signaling. *Front Pharmacol* 8, 953. doi:10.3389/fphar.2017.00953.
- Sun, Y, Yang, J., 2019. A bioinformatics investigation into the pharmacological mechanisms of the effect of Fufang Danshen on pain based on methodologies of network pharmacology. *Sci Rep* 9 (1), 5913. doi:10.1038/s41598-019-40694-4.
- Wang, H, Li, Y, Xia, X, Xiong, X., 2018. Relationship between metabolic enzyme activities and bioaccumulation kinetics of PAHs in zebrafish (*Danio rerio*). *J Environ Sci (China)* 65, 43–52. doi:10.1016/j.jes.2017.03.037.
- Wang, JR, Yau, LF, Tong, TT, Feng, QT, Bai, LP, Ma, J, Hu, M, Liu, L, Jiang, ZH., 2015. Characterization of oxygenated metabolites of ginsenoside Rb1 in plasma and urine of rat. *J Agric Food Chem* 63 (10), 2689–2700. doi:10.1021/acs.jafc.5b00710.
- Wang, JR, Tong, TT, Yau, LF, Chen, CY, Bai, LP, Ma, J, Hu, M, Liu, L, Jiang, ZH., 2016. Characterization of oxygenated metabolites of ginsenoside Rg1 in plasma and urine of rat. *J Chromatogr B Analyt Technol Biomed Life Sci* 1026, 75–86. doi:10.1016/j.jchromb.2015.12.028.
- Wang, JW, Bian, S, Wang, SM, Yang, S, Zhang, WY, Zhao, DQ, Liu, MC, Bai, XY., 2020. Ginsenoside Rh2 represses autophagy to promote cervical cancer cell apoptosis during starvation. *Chin Med* 15 (1), 118. doi:10.1186/s13020-020-00396-w.
- Wang, L, Zhang, Q, Li, X, Lu, Y, Xue, Z, Xuan, L, Wang, Y., 2008. Pharmacokinetics and metabolism of lithospermic acid by LC/MS/MS in rats. *Int J Pharm* 350 (1-2), 240–246. doi:10.1016/j.ijpharm.2007.09.001.
- Wang, X, Wang, C, Pu, F, Lin, P, Qian, T., 2014. Metabolite profiling of ginsenoside Rg1 after oral administration in rat. *Biomed Chromatogr* 28 (10), 1320–1324. doi:10.1002/bmc.3164.
- Wei, Y, Li, P, Wang, C, Peng, Y, Shu, L, Jia, X, Ma, W, Wang, B., 2012. Metabolism of tanshinone IIA, cryptotanshinone and tanshinone I from *Radix Salvia Miltiorrhiza* in zebrafish. *Molecules* 17 (7), 8617–8632. doi:10.3390/molecules17078617.
- Xu, C, Wang, W, Wang, B, Zhang, T, Cui, X, Pu, Y, Li, N., 2019. Analytical methods and biological activities of *Panax notoginseng* saponins: Recent trends. *J Ethnopharmacol* 236, 443–465. doi:10.1016/j.jep.2019.02.035.
- Xu, M, Guo, H, Han, J, Sun, SF, Liu, AH, Wang, BR, Ma, XC, Liu, P, Qiao, X, Zhang, ZC, Guo, DA., 2007. Structural characterization of metabolites of salvianolic acid B from *Salvia miltiorrhiza* in normal and antibiotic-treated rats by liquid chromatography-mass spectrometry. *J Chromatogr B* 858 (1-2), 184–198. doi:10.1016/j.jchromb.2007.08.032.
- Yan, Z, Lu, G, Sun, H, Bao, X, Jiang, R, Liu, J, Ji, Y., 2019. Comparison of the accumulation and metabolite of fluoxetine in zebrafish larva under different environmental conditions with or without carbon nanotubes. *Ecotoxicol Environ Saf* 172, 240–245. doi:10.1016/j.ecoenv.2019.01.089.
- Yang, ST, Wu, X, UPLC/Q-TOF-MS, Rui W., 2015. Analysis for identification of hydrophilic phenolics and lipophilic diterpenoids from *Radix Salviae Miltiorrhizae*. *Acta Chromatogr* 27 (4), 711–728. doi:10.1556/AChrom.27.2015.4.9.
- Yin SJ, Wang YL, Chen H, Hu G, Zheng GC, Yang FQ. Investigation on the metabolism of curcumin and baicalein in zebrafish by liquid chromatography-tandem mass spectrometry analysis 2020; 16(8): 1052-1058. https://doi.org/10.2174/1573412915666190522083850.
- Yu, S, Zhou, X, Li, F, Xu, C, Zheng, F, Li, J, Zhao, H, Dai, Y, Liu, S, Feng, Y., 2017. Microbial transformation of ginsenoside Rb1, Re and Rg1 and its contribution to the improved anti-inflammatory activity of ginseng. *Sci Rep* 7 (1), 138. doi:10.1038/s41598-017-00262-0.
- Zeng, G, Xiao, H, Liu, J, Liang, X., 2006. Identification of phenolic constituents in *Radix Salvia miltiorrhizae* by liquid chromatography/electrospray ionization mass spectrometry. *Rapid Commun Mass Spectrom* 20 (3), 499–506. doi:10.1002/rcm.2332.
- Zeng, GF, Liu, JX, Li, P, Fu, SP, Xiao, HB, Liang, XM., 2006. Protective effects of different ratios of Danshen to Sanqi on hypoxia and reoxygenation-induced HUVECs injury. *Fine Chem* 23 (2), 126–129.
- Zeng, XF, Li, J, Li, Z., 2015. Ginsenoside Rd mitigates myocardial ischemia-reperfusion injury via Nrf2/HO-1 signaling pathway. *Int J Clin Exp Med* 8 (8), 14497.
- Zhang, JY, Liu, MQ, Huang, MH, Chen, MF, Zhang, D, Luo, LP, Ye, GN, Deng, LJ, Peng, YH, Wu, X, Liu, GP, Ye, WC, Zhang, DM., 2019. Ginsenoside F1 promotes angiogenesis by activating the IGF-1/IGF1R pathway. *Pharmacol Res* 144, 292–305. doi:10.1016/j.phrs.2019.04.021.
- Zhang, NN, An, XB, Lang, PP, Wang, F, Xie, YP., 2019. Ginsenoside Rd contributes the attenuation of cardiac hypertrophy in vivo and in vitro. *Biomed Pharmacother* 109, 1016–1023. doi:10.1016/j.biopha.2018.10.081.
- Zhao, WJ, Huang, MR, Shang, ZP, Wang, ZJ, Wang, ZB, Zhang, JY., 2018. Metabolites of tanshinone I and tanshinone IIA in vivo in rats. *Zhongguo Zhong Yao Za Zhi* 43 (1), 174–182. doi:10.19540/j.cnki.cjcm.2018.0005.
- Zhou, X, Razmovski-Naumovski, V, Kam, A, Chang, D, Li, C, Bensoussan, A, Chan, K., 2017. Synergistic effects of Danshen (*Salvia Miltiorrhizae Radix* et *Rhizoma*) and Sanqi (*Notoginseng Radix* et *Rhizoma*) combination in angiogenesis behavior in EAhy 926 cells. *Medicines (Basel)* 4 (4), E85. doi:10.3390/medicines40400085.
- Zhou, X, Razmovski-Naumovski, V, Kam, A, Chang, D, Li, CG, Chan, K, Bensoussan, A., 2019. Synergistic study of a Danshen (*Salvia Miltiorrhizae Radix* et *Rhizoma*) and Sanqi (*Notoginseng Radix* et *Rhizoma*) combination on cell survival in EA.hy926 cells. *BMC Complement Altern Med* 19 (1), 50. doi:10.1186/s12906-019-2458-z.